BNL-212313-2019-TECH

NSLSII-ASD-TN-320

NSLS-II FOFB Performance Improvement in 2019

S. Kongtawong

October 2019

Photon Sciences

Brookhaven National Laboratory

U.S. Department of Energy

USDOE Office of Science (SC), Basic Energy Sciences (BES) (SC-22)

DISCLAIMER

NSLS-II TECHNICAL NOTE BROOKHAVEN NATIONAL LABORATORY	NUMBER **NSLSII-ASD-TN-320**
AUTHORS: S. Kongtawong, X. Yang, K. Ha, Y. Tian, L. Hua Yu, J. Ricciardelli, D. Padrazo, M. Maggipinto, T. Shaftan	DATE 10/31/2019
NSLS-II FOFB Performance Improvement in 2019	

NSLS-II FOFB performance improvement in 2019

Sukho Kongtawong[1], Xi Yang[2], Kiman Ha[2], Yuke Tian[2], Li Hua Yu[2], John Ricciardelli[2], Danny Padrazo[2], Marshall Maggipinto[2], and Timur Shaftan[2]

[1]Department of Physics and Astronomy, Stony Brook University, NY 11794-3800, USA
[2]NSLS-II, Brookhaven National Laboratory, Upton, NY 11973, USA

Motivation

APS-U declared that they have achieved 700 Hz to 1kHz fast orbit feedback (FOFB) close-loop bandwidth in their two-section test setup [1]. Before this, most light sources have been running FOFB with 100-200Hz bandwidth. Table. 1 shows the information of bandwidths and sampling rates of various Synchrotron facilities [2-8].

Table 1: FOFB bandwidths and sampling rates of various SR facilities

SR Facility	sampling rate of FOFB (kHz)	Bandwidth (Hz)
ALS	1.11	60
APS	1.6	80
BESSY-II	2.4	40
ALBA	5	~100
DIAMOND	10	130
ESRF	10	150
APS-U	22.6	700 - 1000

NSLS-II FOFB has been running with 250 Hz close-loop bandwidth since the FOFB commissioning in 2015 [9]. Based on the figure-of-merit estimation, the FOFB bandwidth in NSLS-II should be close to $f_{sam}/20$ = 10,000 Hz/20 = 500 Hz. A factor of two difference in the FOFB bandwidth is not accidental. We need to understand where this discrepancy comes from and therefore optimize the FOFB system to reach a higher FOFB bandwidth. Since NSLS-II is a user facility, we must optimize the FOFB without affecting the normal user operation.

Methods

Simulated BPM button signals

To measure the performance of BPM and FOFB, we need to generate simulated BPM button signals in the lab. Fig. 1 shows such a system.

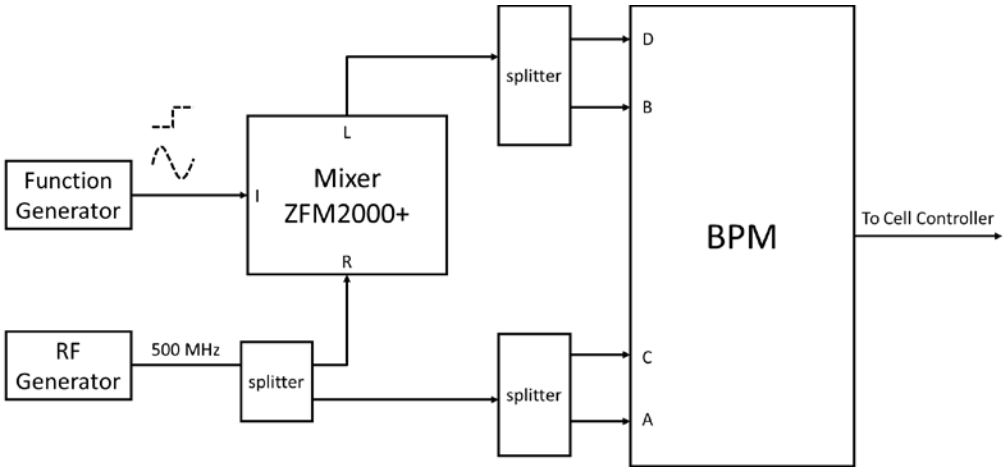

Figure 1: Diagram shows a circuit to generate a simulated BPM button signal.

A RF generator is used to create a RF signal at 499.68 MHz. With two RF splitters, two copies of this signal are feed into BPM as A and C button signals. The other signal from the first splitter goes to the RF input of a RF mixer. The input of the mixer comes from a function generator, which can produce any shape of the signal e.g. cosine wave, square wave. This way, we can generate any shape of the input into the BPM. Fig. 2 shows the data that BPM reads from the square wave and sine wave input.

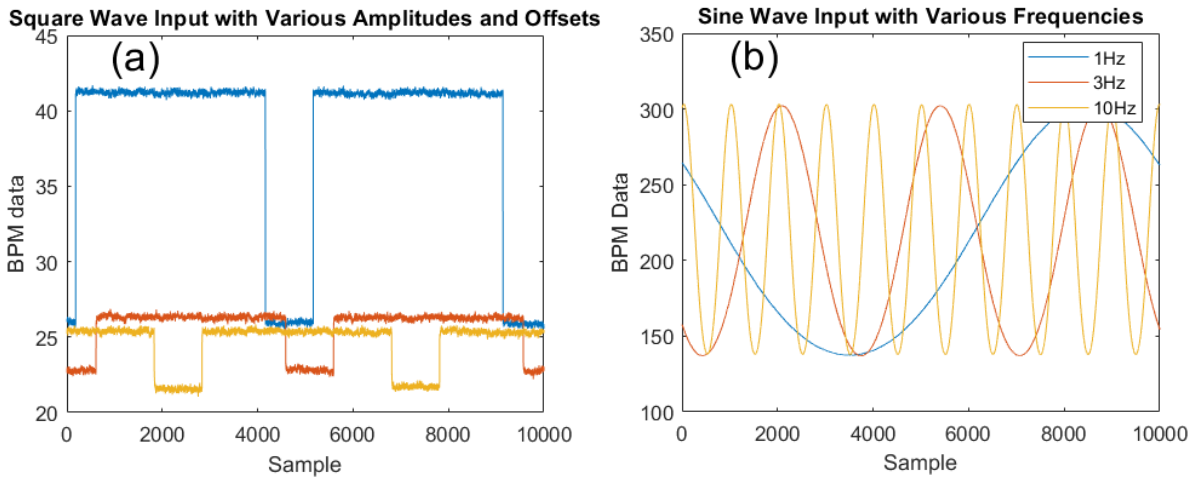

Figure 2: Data read from BPM when we fed square (a) and sine (b) waves into the input.

This system can be used in the lab. It can also be used in the storage ring to measure the latency and transfer function without electron beam.

Measurement of the latencies from different sections of FOFB

Latencies in FOFB are critical for the performance. It is desirable to measure the latency in each section of the FOFB and to make sure all latencies are minimized. Our first latency measurement focus on the BPM, cell controller, power supply controller (PSC) and power supply interface (PSI). It is shown as the section of the dashed line and above in Figure 3. The function generator created a simulated BPM signal. The signal is distributed to all cell controllers through SDI link. The cell controller performs FOFB calculation and sends the fast corrector setpoints to the power supply controller (PSC) and the power supply interface (PSI).

In this measurement, the function generator signal is the reference signal. It goes to the first channel of an oscilloscope. We added a DAC chip in BPM to measurement the BPM FA data as an analog format. This BPM signal goes to the 2^{nd} channel of the oscilloscope. The Cell controller can output two analog signals, one before the FOFB calculation (or called SDI data) and the other after the FOFB calculation. These two can go to the 3^{rd} and 4^{th} channels of the oscilloscope. Last, the fast corrector PSI has a DAC signal to represent the setpoint. This signal can go to 5^{th} channel of the oscilloscope. With these 5 signals, we can check all the latencies from BPM to PSI. The above BPM-to-PSI latency measurement can be done in the lab as well as in the storage ring. We did both for the cross check.

The BPM-to-PSI latency measurement does not include the latency of the power supply regulator, the power amplifier, the magnet, the vacuum chamber, and the beam delay. To measure this latency, we need the real beam. The measurement is shown in the all solid line section in Figure 3. We use the function generator (instead of PSI DAC output) to directly drive the power supply regulator, which drives the power amplifier and fast corrector. The fast corrector kicks the beam. The rest measurement is the same as described above. This measurement provides the latency in the regulator, power amplifier, magnet, vacuum chamber and the beam itself.

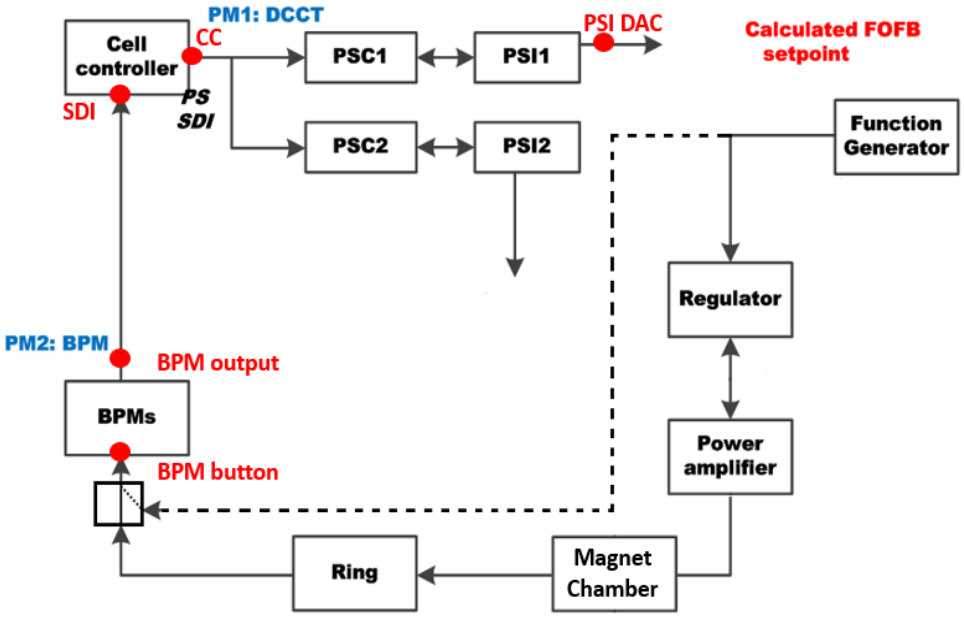

Figure 3: Schematic of the experimental setup for the FOFB latency/transfer function measurement in the storage ring.

The FOFB system is running with a machine clock at 10 kHz. The periodic step functions generated by the function generator are running freely and it is **asynchronous** with respect to the machine clock. Therefore, there always exists a systematic timing jitter anywhere between 0 up to a machine clock 100 µs due to the asynchronization. We measure the stage-by-stage delay by simply searching the minimal delay between the drive signal and the signal at every stage. The persistent mode of the scope is used to find the minimum delay in the measurement therefore removing the extra delay caused by the asynchronous function generator signal.

Characterize the bandwidth of the FOFB system with fast and slow methods

We use two different methods to characterize the gain and bandwidth of the FOFB system. Power spectral density (PSD) at different frequencies are used to compare FOFB- on and off conditions (named as the on-off ratio). Routinely, the bandwidth is determined by the crossover frequency where this on-off ratio is one, or unit gain. It means that the noise above this frequency instead of being suppressed is excited

The FOFB on/off PSD method is fast but not precise. Since the perturbations to the beam come from the environmental sources, such as ground motion, utility water pump, etc., the sources at some frequencies are weak and fundamentally limit the measurement precision. The 2nd method is slow but with higher precision. In this method, we intentionally generate a narrow bandwidth noise to the beam by simply driving a fast corrector using a simulated sine-wave. Both BPM and the cell controller can generator such a sine-wave. It can also be generated using a

function generator. By doing so, the beam is perturbed by a controllable amplitude at different frequencies. For different frequency, we can measure the PSD with FOFB on and off to get the FOFB performance at different frequencies. Since the noise is narrowband and the amplitude is much larger than the nature noise, the FOFB performance measurement precision can be greatly improved. The only drawback is this method is time consuming.

Local FOFB mode

NSLS-II is an operational machine. Any upgrade needs to be done cell-by-cell and carefully examined afterward. Local FOFB mode is implemented to serve such purpose. In this special mode, we only include fast correctors and BPMs in those relevant sections to perform the FOFB function while the remaining fast correctors and BPMs are disabled from the FOFB loop. The routine procedures - perform SVD with valid fast correctors and BPMs; download U^T and V matrix to each cell controller (CC); take reference orbit; setup fast correctors to FOFB mode; setup SDI communication is valid for both standard and local FOFB modes. When we upgrade the software and firmware in the FOFB, such as BPM, cell controller, PSC, and PSI, we always use local FOFB mode to compare the FOFB performances of cells with updated firmware with cells with original firmware.

Results

Latency and transfer function measurement in the lab

We measured the step response and the transfer function of the system in the lab and created a model of the subsystem (without the beam). The step response can be measured by feeding square wave into the BPM and measure the output from different stages which are the BPM DAC, CC DAC, and PSI outputs. Fig. 4(a) shows an example of the step response from BPM to CC DAC and a theoretical model with a delay of 250 us. The open-loop transfer function can be measured by feeding sine waves and varying the frequency of the input. Fig. 4(b) shows the measured (circles) and modeled (blue curve) transfer functions of this stage. The model fits well with the data. The simulation and modeling of the system by using control theory are discussed in another report [10].

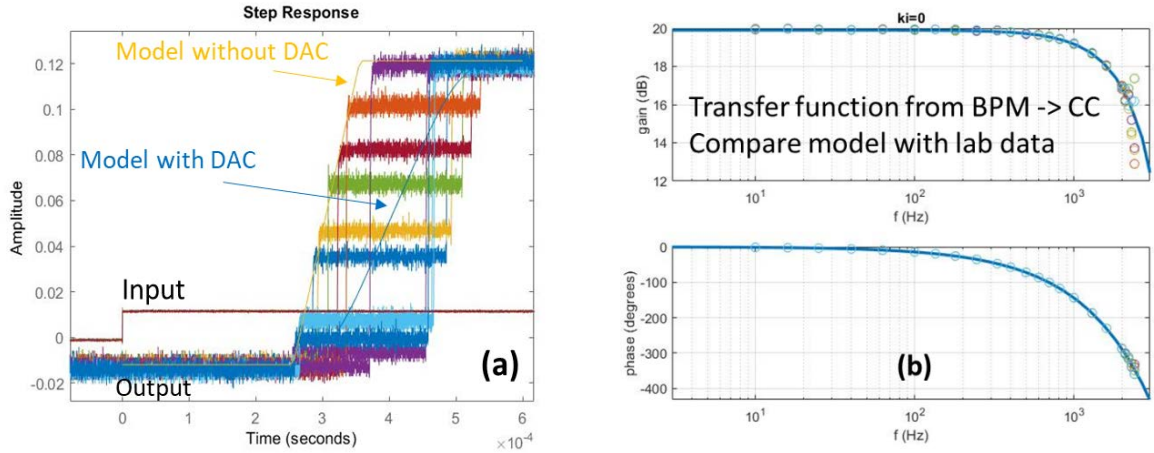

Figure 4: (a) Step response of the system from BPM to Cell Controller DAC measured in the lab compare with the model and (b) The transfer function of the same system

Latency measurement of the real system

We measured the FOFB open-loop latency of the storage ring in a beam study. One fast corrector in cell 28 was driven by the external function generator. The orbit was therefore perturbed (described in detail in the Methods section). With the FOFB matrix downloaded in each CC and the fast correctors set in non-FOFB mode, we placed the FOFB system in the open-loop mode. We measured the latency between the external driving signal and the open-loop signal at each stage with a breakpoint, including BPM button, BPM output, SDI, CC, and PSI DAC, shown as red dots in Fig. 3.

The total latency of the FOFB system, starting from the fast corrector power supply output ending at PSI DAC (Fig. 3), was about 350us. The detail distribution of measured latencies was 70 µs in the storage ring, **115 µs** from BPM, 30µs from SDI link, **105 µs** from matrix calculation in the cell controller and 30 us from CC to PS. The total is 70 + **115** + 30 + **105** + 30 = 350 µs from breakpoints of BPM button to the PSI output. Two leading contributors, BPM button to output and CC, were suspected and highlighted as bold numbers above.

BPM firmware update with latency reduction of 100 µs

It was found that the BPM latency 115 µs, which is the delay between the BPM RF button signal and the BPM data output, can be reduced by one machine clock, 100 µs. The new firmware in the lab has been tested and confirmed. The latency for the new firmware was reduced to <20 us (see Fig. 5).

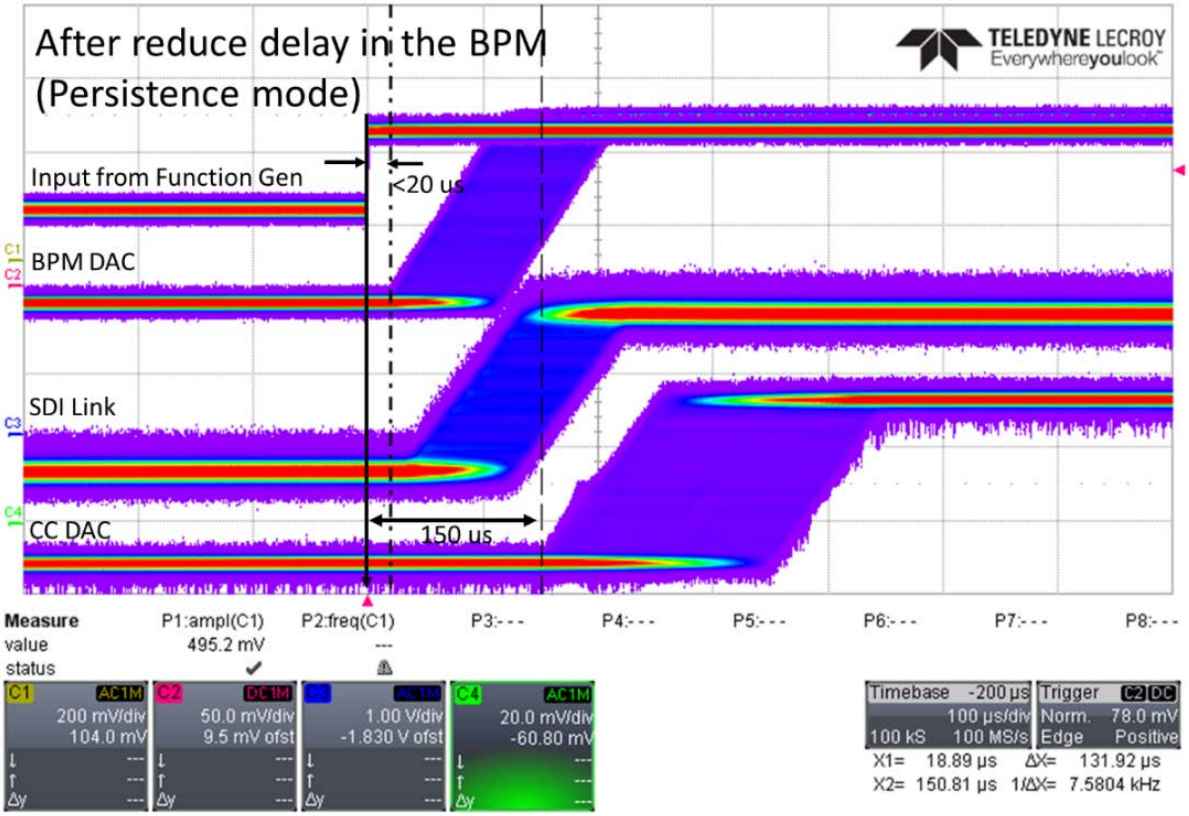

Figure 5: Shows latency measurement of each stage from the input, BPM output, SDI link, and Cell Controller DAC.

Kiman and diagnostic group upgraded the 18 BPMs in cell 13-15 with the new low-latency firmware. After the upgrade, we repeated the same latency measurement with the beam to confirm the reduction of the latency. The total latency was reduced to 250 µs in cell 13-15, comparing to 350 µs at the rest cells with old BPM firmware. Screen captured scope latency measurements were shown in Fig. 6 (a) and (b) with respect to before and after the upgrade.

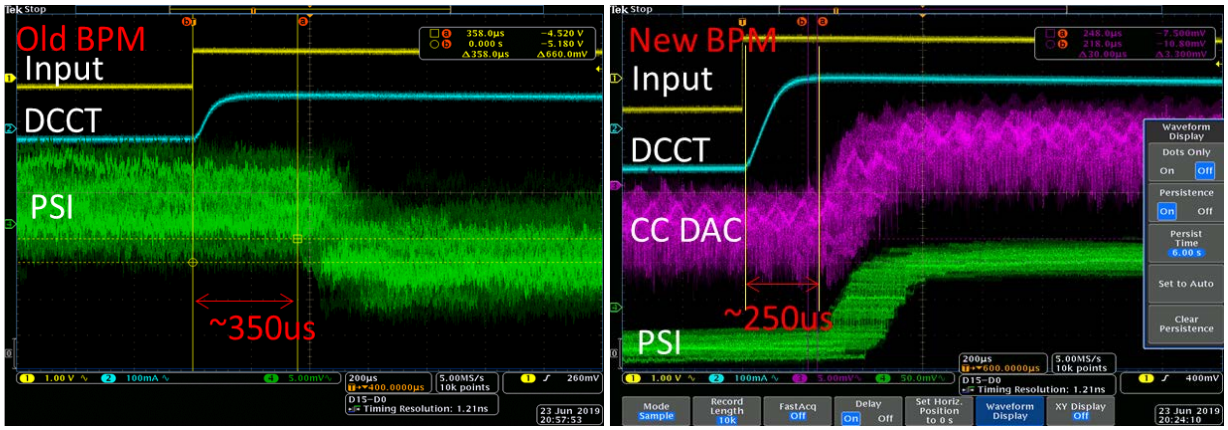

(a) (b)

Figure 6: Delay measurement before (a) and after (b) installing the new BPM firmware to reduce the 100 μs latency.

We must evaluate the impact of the latency reduction caused by the new BPM firmware before upgrading all the BPMs. To study the BPM latency effect, we applied the local FOFB mode which only included the BPMs and fast correctors in Cell 13 to 15. In addition to measurement the PSD function at different excited frequencies when FOFB on and off, we measured the PID parameters at which the orbit started oscillating. We kept increasing Kp (proportional controller parameter) until the system became unstable. When Kp was increased to 900, the system started oscillating. We recorded 10 seconds of FA data of all BPMs.

Similarly, we only used BPMs and fast correctors in C16 to C18 in FOFB. When the Kp parameter was increased to 800, the system started oscillating. The fact that latency-reduced BPM enabling the FOFB system with a higher Kp value implies that FOFB bandwidth has been improved. With the Kp value of 900, both FOFB configurations were oscillating, but the FOFB with the low-latency BPMs have a factor of five smaller oscillating amplitude. Besides, the amplified peak at 740 Hz (before the BPM firmware upgrade) was moved to 928 Hz (after this upgrade). It also indicates the increase of the FOFB bandwidth. The PSD comparison is shown in Fig. 7.

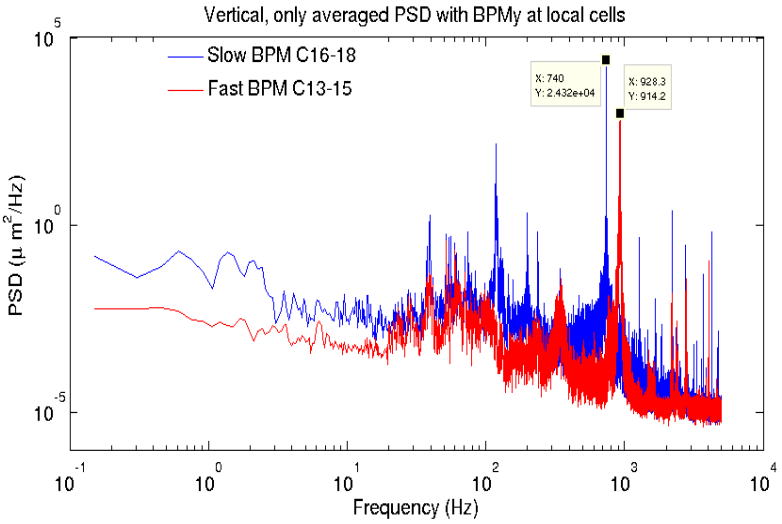

Figure 7: Comparing PSDs in the vertical direction before (blue) and after (red) the BPM firmware upgrade at the same FOFB setting parameters, the amplified peak at 740 Hz (before) was moved to 928 Hz (after). It indicates the increase of the FOFB bandwidth.

After the beam-based confirmation of the bandwidth improvement, all BPMs were upgraded with the low-latency firmware in July 2019. We performed the bandwidth characterization of the FOFB system using the slow and precise method described in the section

of Methods. The results were compared to the data taken before the BPM firmware upgrade. Gain *vs* frequency in the horizontal and vertical directions are plotted as Figs. 8 (a) and (b) respectively. The comparison of before (red) and after (blue) the BPM upgrade indicates the horizontal bandwidth increases from 250 Hz to 350 Hz and the vertical bandwidth increases from 200Hz to 300Hz. Several beamlines noticed the FOFB performance improvement and they commended the upgrade.

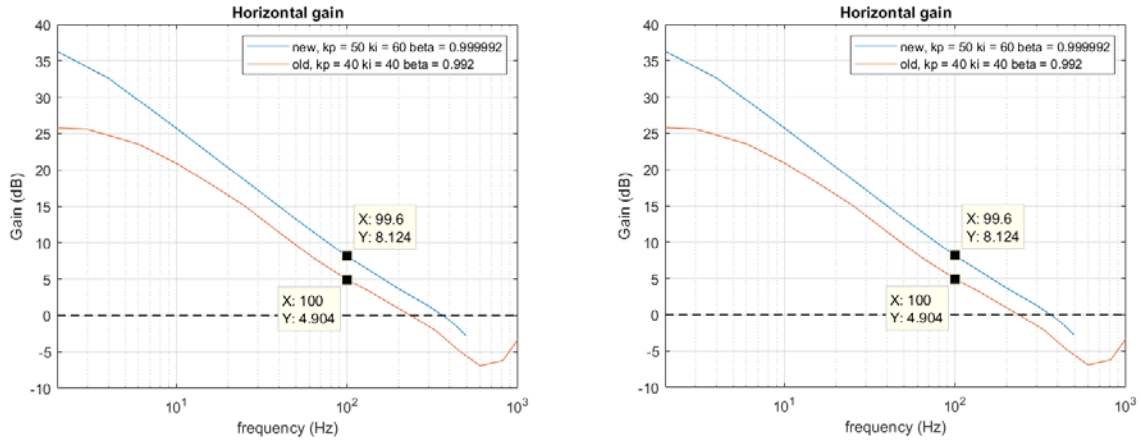

(a) (b)

Figure 8: (a) Horizontal gain vs frequency before (red) and after (blue) the BPM firmware upgrade and (b) Vertical gain vs frequency

Cell controller firmware update with 10 kHz output and latency reduction of 30 µs

The next effort was to reduce the latency from cell controller. Based on the latency measurement shown in Fig. 9, the signal after CC became 5 kHz.

Figure 9: The 10 kHz machine clock becomes 5 kHz at the breakout point of CC (blue).

In the early commissioning stage in 2005, the FOFB matrix calculation took 105us. To make sure the other function of the cell controller, active interlock system, to work reliably, the

FOFB system clock was reduced to 25 MHz. The FOFB calculation update period was increased to 200 us (5 kHz). Meanwhile, the BPM data transmission through SDI link was kept 10kHz, and power supply control rate was also 10kHz. This configuration has been kept till now we are starting to make the improvement.

With the AI system more mature and well defined, we can now reliably increase the internal system clock from 25MHz to 50MHz. Therefore, the FOFB setpoint update rate is increased to 10kHz.

Similarly, we need to confirm the FOFB performance with the new cell controller firmware using local FOFB mode. To do this, we sequentially configured the FOFB in local mode at two different sections, one with the old CC firmware in C20-22 and the other with the upgraded firmware in C24-26. A quick test was done by setting kp = 1000. Both FOFB configurations were oscillating in the horizontal plane, but the amplified peak at 1069 Hz in the C20-22 configuration was moved to 1512 Hz in the C24-26 configuration. Similarly, Both FOFB configurations were oscillating in the vertical plane with kp = 3000, but the amplified peak, instead of at 716 Hz, was moved to 1245 Hz after the CC upgrade. This measurement indicates the increase of the FOFB bandwidth due to new cell controller firmware. The results are shown in Fig. 10.

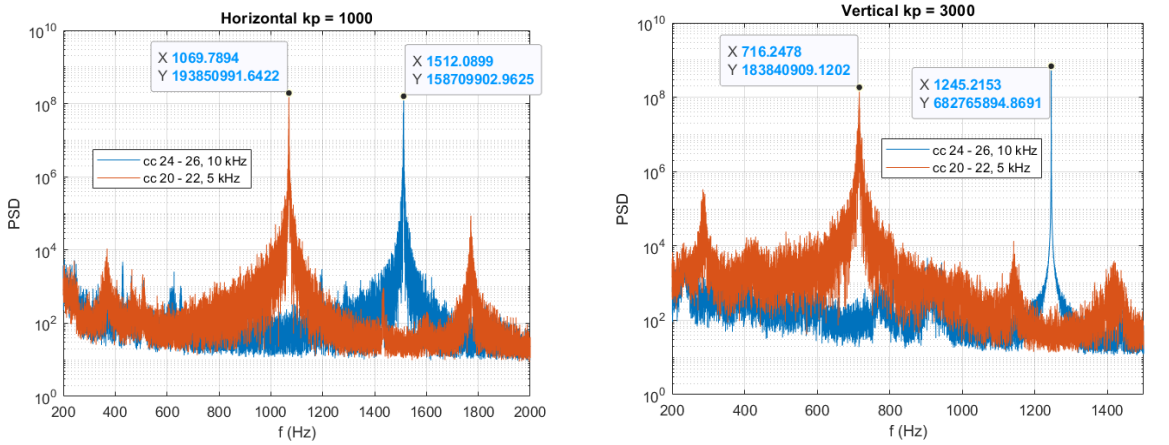

(a) (b)

Figure 10: Comparing PSDs in the horizontal (a) and vertical (b) directions before (orange) and after (blue) the CC firmware upgrade.

Detail information of the stage-to-stage delay in the FOFB system (row) and the history of the improvements (column) is shown in Fig. 11. Note that the calculation time that we expected should be around 50 us which is reduced from 100 us. However, we measured the latency and found that the latency reduced by only about 30 us. The source of the 20 us latency still is a question.

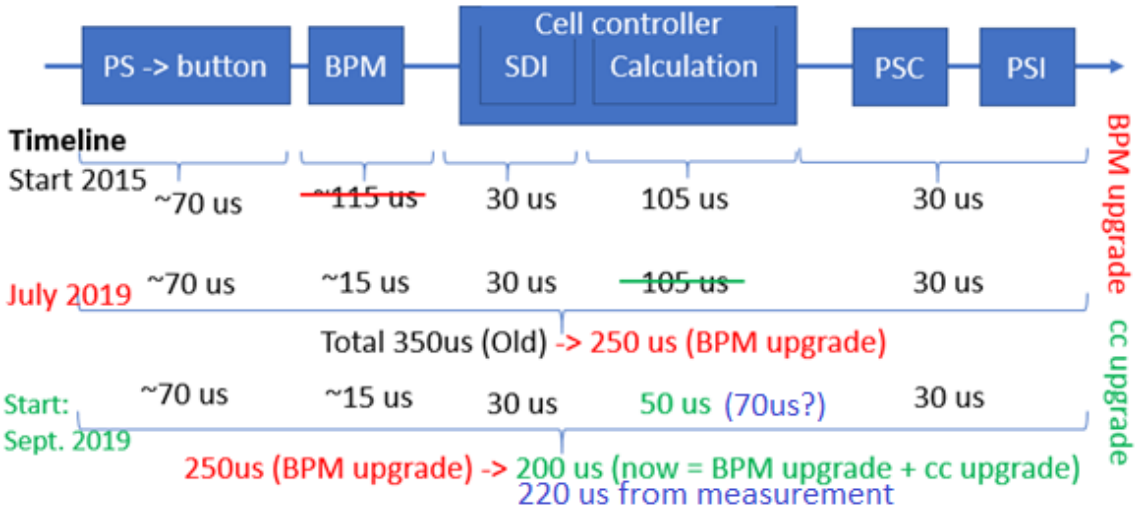

Figure 11: Detail of the stage-to-stage delays in FOFB (row) and the improvement history (column).

Summary and Discussion

We implemented a standard stage-to-stage latency characterization method for the FOFB system. This method has been proved to be extremely effective in diagnosing errors in the FOFB system and providing insights on how to fix those issues. Based on the latency measurement, we found two leading contributors to the system: extra 100us delay in BPM firmware, and a slowdown of FOFB calculation. We have upgraded all the BPM firmware to successfully fix one of the problems. The bandwidth of the FOFB system has been increased 40% in H plane and 50% in V plane after the upgrade. We are in the process of upgraded CC firmware. Further improvement is expected after the completion of the CC upgrade.

We tested two different ways to characterize the bandwidth of the FOFB system. One is traditional On/Off PSD comparison without orbit excitation. This method is fast but with low precision. The second method, PSD compare with orbit excitation, is slower but with higher accuracy. The second method was applied to build the FOFB model with a reasonably good agreement with the machine performance. As an example, the model predicted gain (top) and phase (bottom) *vs* frequency (blue curve) agrees well with the measurement (orange circles), as shown in Fig. 12. Therefore, we can apply the model to optimize machine performance in the future.

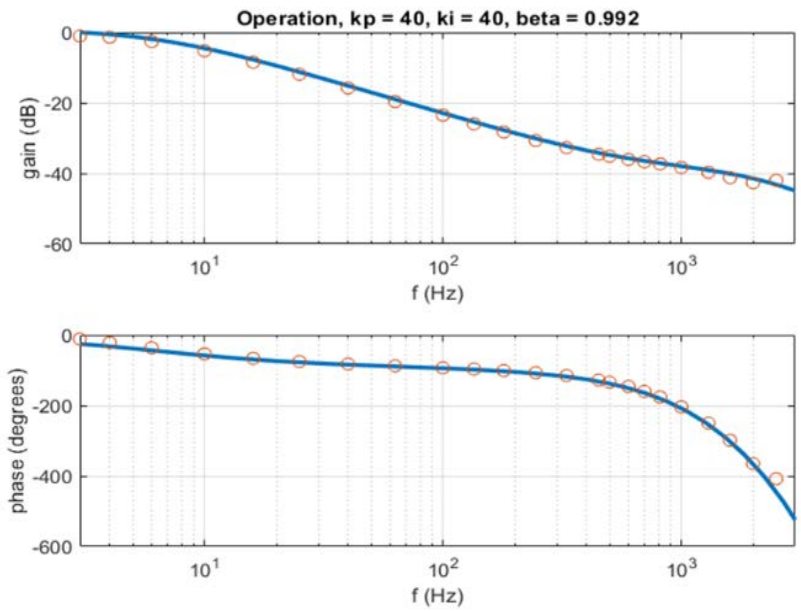

Figure 12: The model based on equation $G = k_p + k_i/(1-\beta z^{-1})$ of 5 kHz sampling rate is perfectly fit with the experimental data.

Future works

While we have addressed the two main latency issues in the FOFB system, the FOFB performance is clearly improved. The remaining optimization work for the FOFB mainly included optimization of PID parameters, compare the theoretical model with the real machine and online optimization. The following list reflects some of the future works.

1. Upgrade all CC to 10kHz version
2. Optimize kp and ki for a new operation with 10 kHz
3. Measure gain/bandwidth and the transfer function of the new system
4. Optimize kp, ki of different modes
    a. Theory and model
    b. Online optimization
5. Optional: add a notch filter to the calculation (minor thing)
6. Work on the ORM modification, the gain of BPM, errors of the feedback system

Acknowledgement

We would like to thank Beam Diagnostic group and Power Supply group for very helpful supports and technical suggestions.

References

[1] Advanced Photon Source Upgrade Project Preliminary Design Report, Chapter 4: Accelerator Upgrade, September, 2017

[2] N. Hubert, *et al.,* “GLOBAL ORBIT FEEDBACK SYSTEMS DOWN TO DC USING FAST AND SLOW CORRECTORS”, DIPAC09, Basel, Switzerland, 2009.
[3] C. Steier, E. Domning, T. Scarvie, and E. Williams, “OPERATIONAL EXPERIENCE INTEGRATING SLOW AND FAST ORBIT FEEDBACKS AT THE ALS”, EPAC 2004, Lucerne, Switzerland, 2004.
[4] J. Carwardine, *et al*., “APS UPGRADE INTEGRATED BEAM STABILITY EXPERIMENTS USING A DOUBLE SECTOR IN THE APS STORAGE RING”, International Beam Instrumentation Conference, Shanghai, 9-14 September 2018.
[5] R. Muller, *et al*., “INSTALLING A FAST ORBIT FEEDBACK AT BESSY”, IPAC’10, Kyoto, Japan, 2010.
[6] A. Olmos, *et al*., “COMMISSIONING OF THE ALBA FAST ORBIT FEEDBACK SYSTEM”, IBIC2014, Monterey, CA, USA, 2014.
[7] M. G. Abbott, *et al*., “PERFORMANCE AND FUTURE DEVELOPMENT OF THE DIAMOND FAST ORBIT FEEDBACK SYSTEM”, EPAC08, Genoa, Italy, 2008.
[8] E. Plouviez, F. Epaud, J.M. Koch, and K.B. Scheidt, “THE NEW FAST ORBIT CORRECTION SYSTEM OF THE ESRF STORAGE RING”, DIPAC2011, Hamburg, Germany, 2011.
[9] Y. Tian, *et al*., “NSLS-II FAST ORBIT FEEDBACK SYSTEM”, ICALEPCS2015, Melbourne, Australia, 2015
[10] Not published yet